Chin. J. Astron. Astrophys. Vol. 5 (2005), No. 5, 531–538
(*http://www.chjaa.org*)

Chinese Journal of
Astronomy and
Astrophysics

Polar Coronal Holes During Solar Cycles 22 and 23

Jun Zhang[1,2], J. Woch[2] and S. Solanki[2]

[1] National Astronomical Observatories, Chinese Academy of Sciences, Beijing 100012
zjun@ourstar.bao.ac.cn
[2] Max-Planck-Institut für Sonnensystemforschung, Katlenburg-Lindau, D-37191, Germany

Received 2005 April 18; accepted 2005 July 2

Abstract Data from the Solar Wind Ion Composition Spectrometer (SWICS) on Ulysses and synoptic maps from Kitt Peak are used to analyze the polar coronal holes of solar activity cycles 22 and 23 (from 1990 to end of 2003). In the beginning of the declining phase of solar cycles 22 and 23, the north polar coronal holes (PCHs) appear about one year earlier than the ones in the south polar region. The solar wind velocity and the solar wind ionic charge composition exhibit a characteristic dependence on the solar wind source position within a PCH. From the center toward the boundary of a young PCH, the solar wind velocity decreases, coinciding with a shift of the ionic charge composition toward higher charge states. However, for an old PCH, the ionic charge composition does not show any obvious change, although the latitude evolution of the velocity is similar to that of a young PCH.

Key words: Sun: coronal — Sun: particle emission — Sun: solar wind

1 INTRODUCTION

Non-transient solar wind varies in many respects both in time and space. This is outstandingly reflected in the transition from its bimodal nature during solar minimum with fast wind emanating from the polar regions and slow wind from lower latitudes to a continuum of dynamic states (Zurbuchen et al. 2002) during solar maximum.

The variations manifest themselves not only in the solar wind speed but, moreover, in considerable differences in the charge-state distribution of heavy elements between the fast and slow solar winds (von Steiger et al. 1997). It is generally assumed that the charge-state distribution is mainly determined by the electron temperature profile of the lower solar corona. Therefore, measurements of the charge-state composition in interplanetary space can provide information on the physical conditions in the source regions of the solar wind.

It was suggested that different source regions at the Sun produce different types of solar wind (Schwenn, Mülhauser & Rosenbauer 1981). The fast solar wind originates from coronal holes (Krieger et al. 1973). During the minimum of the solar activity cycle, fast solar wind streams emanating from large-scale polar coronal holes (PCHs) dominate the solar wind distribution in

the heliosphere (e.g., Woch et al. 1997). Recent observations suggested the magnetic transition region network in PCH as the source region of the fast solar wind (Hasisler et al. 1999).

McComas et al. (2000) used Ulysses solar wind plasma and ion composition data to study a limited number of solar wind streams assumed to emanate from small-scale coronal holes which existed at high latitudes near solar maximum. They found that the ionic composition of these streams is comparable to that of the wind emanating from the polar hole wind. They concluded that coronal holes, regardless of whether they are small-scale solar maximum ones or large-scale polar minimum holes, produce a unique type of solar wind. Zhang et al. (2003) partly corroborated this result by analysing a larger number of maximum holes. However, they also showed that solar maximum holes with a magnetic polarity of the previous solar cycle may differ significantly in their ionic composition from the polar coronal holes. Many of the old-polarity-holes show a considerably higher coronal temperature. Zurbuchen et al. (2002) used Ulysses/SWICS data to examine the evolution of the solar wind composition throughout the solar cycle. They reported a higher charge-state ratio in coronal-hole-associated wind during solar maximum and concluded that this is consistent with theories in which the solar wind originates from closed magnetic loops that reconnect with open field lines (Fisk et al. 1999).

During the declining and minimum phase of solar cycle 22, there were two polar coronal holes and the kinetic properties of the solar wind emanating from them did not differ significantly. However, the electron temperature in the two coronal holes inferred from ionic charge composition data showed consistent differences, with the south polar hole 10 to 15% hotter. The ground-based magnetograms show that the flux density of the north polar coronal hole was considerably lower for the whole interval of time between 1992 and 1997 (Zhang et al. 2002). The coronal temperature of small-scale coronal holes from the rising to the maximum phase of cycle 23 were constrained by the magnetic polarity of the coronal holes. Whereas newly emerging coronal holes with the polarity of the new cycle did not show any significant difference to the temperatures of the polar minimum holes, those with the polarity of the old cycle showed a considerably enhanced temperature. Regardless of polarity, solar wind streams emanating from small-scale holes generally had lower velocities of 400 to 600 km s^{-1} compared to the polar hole stream velocities of 700 to 800 km s^{-1}. This striking discrepancy in their kinetic properties may partly be attributed to effective deceleration of the fast solar wind from small-scale holes during its propagation to the spacecraft, caused by its interaction with the ambient slow solar wind (Zhang et al. 2003).

In this paper, we investigate PCHs during solar cycles 22 and 23. Using data from the SWICS instrument on Ulysses, we identify coronal hole streams in interplanetary space and relate them to coronal holes seen in Kitt Peak synoptic maps. Specifically, we concentrate on the latitudinal evolution of the O^{7+}/O^{6+} charge state ratio and the solar wind speed in solar wind streams emanating from PCHs. The variation of the speed and the charge-state ratio from the center to the boundary of a PCH is studied.

2 OBSERVATIONS

Data from the Solar Wind Ion Composition Spectrometer (SWICS) aboard Ulysses are used to derive the solar wind proton speed and the charge-state ratio of O^{7+}/O^{6+} as a proxy for the coronal temperature. The study is based on data collected between 1992 and 2003. The SWICS instrument is described in detail by Gloeckler et al. (1992), and a method to derive the O^{7+}/O^{6+} ratio including instrumental errors, by von Steiger et al. (2000). The instrument is well suited to determine the mass and mass per charge of heavy solar wind ions as well as the proton and alpha particle speed, density, and temperature. The O^{7+}/O^{6+} ratio can be used to estimate the so-called freezing-in temperatures which are related to coronal temperatures in the source region of the solar wind. Specifically, in fast coronal hole streams the charge-state

ratio is a most suitable indicator of the coronal temperature (Geiss et al. 1995; von Steiger et al. 2000).

The Ulysses observations are complemented by basic parameters like the coronal hole area, coronal hole magnetic flux and density derived from ground coronal hole maps and magnetograms. The maps of coronal holes by Carrington rotation number are inferred from 1083 nm He I observations made at Kitt Peak. The synoptic maps were constructed from strips along the central meridian of daily maps of the sun. The original observations were made with 1 arcsec pixels and then converted to daily, low resolution maps in a Carrington longitude vs. sine latitude format. Each of the synoptic maps represents one Carrington rotation of the Sun.

The following corrections are applied to the magnetic synoptic charts. (1) On the generally made assumption that the fields are perpendicular to the solar surface, the observed fields are divided by the cosine of the latitude. (2) Magnetograph signals very close to the poles can be very noisy or even missing. In these cases we replaced the measured signal by a cubic spline fit to the valid values in the polar regions. Coronal hole boundaries are identified on the He I 1083 nm synoptic maps, from which the polar coronal hole areas are estimated. Within the coronal hole boundaries the net magnetic flux and net flux density are derived from the magnetic synoptic maps.

The solar wind emanating from the polar coronal holes is uniquely characterized by a high solar wind velocity and a low frozen-in temperature. The rise in solar wind speed and the corresponding drop in the O^{7+}/O^{6+} ratio occurs on short time scales within a few measurement cycles of the instrument, thus yielding sharp boundaries at the interfaces between the coronal hole streams and the ambient solar wind. Figure 1 shows the variation of the charge-state ratio and the solar wind velocity in the 4-year interval from 2000 to end of 2003. The use of 15-hour averaged values was required to sufficiently reduce statistical uncertainties in the O^{7+}/O^{6+} ratio. During the first part of the displayed interval Ulysses encounters several short duration coronal hole streams emanating from small-scale coronal holes emerging at mid to low latitudes during the maximum activity phase of cycle 23. From the beginning of 2001 onwards Ulysses encounters the newly formed north polar coronal hole. Initially, Ulysses is within the stream for only short periods of time during each solar rotation. Then, from June 2001 onward the spacecraft is continuously embedded in the fast coronal hole stream for several months until November 2001. During this period Ulysses was at its highest northern latitudes. Thereafter, with Ulysses moving to lower latitudes, we have another period of only short encounters. Ulysses observed several prominent fast streams emanating from small-scale, mid-to-low latitude coronal holes up to the end of the displayed interval. In the 2nd half of 2003 a series intense coronal mass ejections occurred which influenced strongly the overall solar wind pattern.

The heliographic latitude range scanned by Ulysses from late 1990 to mid-2003 and the variation of solar activity represented by the sunspot number (from early 1990 to mdi-2003) are shown in Figure 2a. During the declining phase of solar cycle 22, Ulysses was at southern heliographic latitudes, and reached the highest southern latitude of 80° in 1994. The fast latitude scan in 1994/1995 at perihelion took Ulysses in just a few months from the south into the north polar regions of the Sun. During the minimum phase of the solar cycle 22 Ulysses descended from high northern latitudes towards the ecliptic and began its second pole to pole scan.

Figure 2b gives an overview of the O^{7+}/O^{6+} charge-state ratio and the solar wind proton speed measured by SWICS in the south and north PCH streams during solar cycles 22 and 23. Displayed are the values of the speed and the O^{7+}/O^{6+} charge-state ratio averaged over 15 hours for each Carrington rotation. The value is taken at the time of maximum speed (CME intervals are excluded). In this way it is made sure that specifically for mid-latitude observations, when Ulysses encountered the polar streams once per rotation for a limited time only, the core of the stream is considered. The speed of the solar wind from the two north and south PCHs

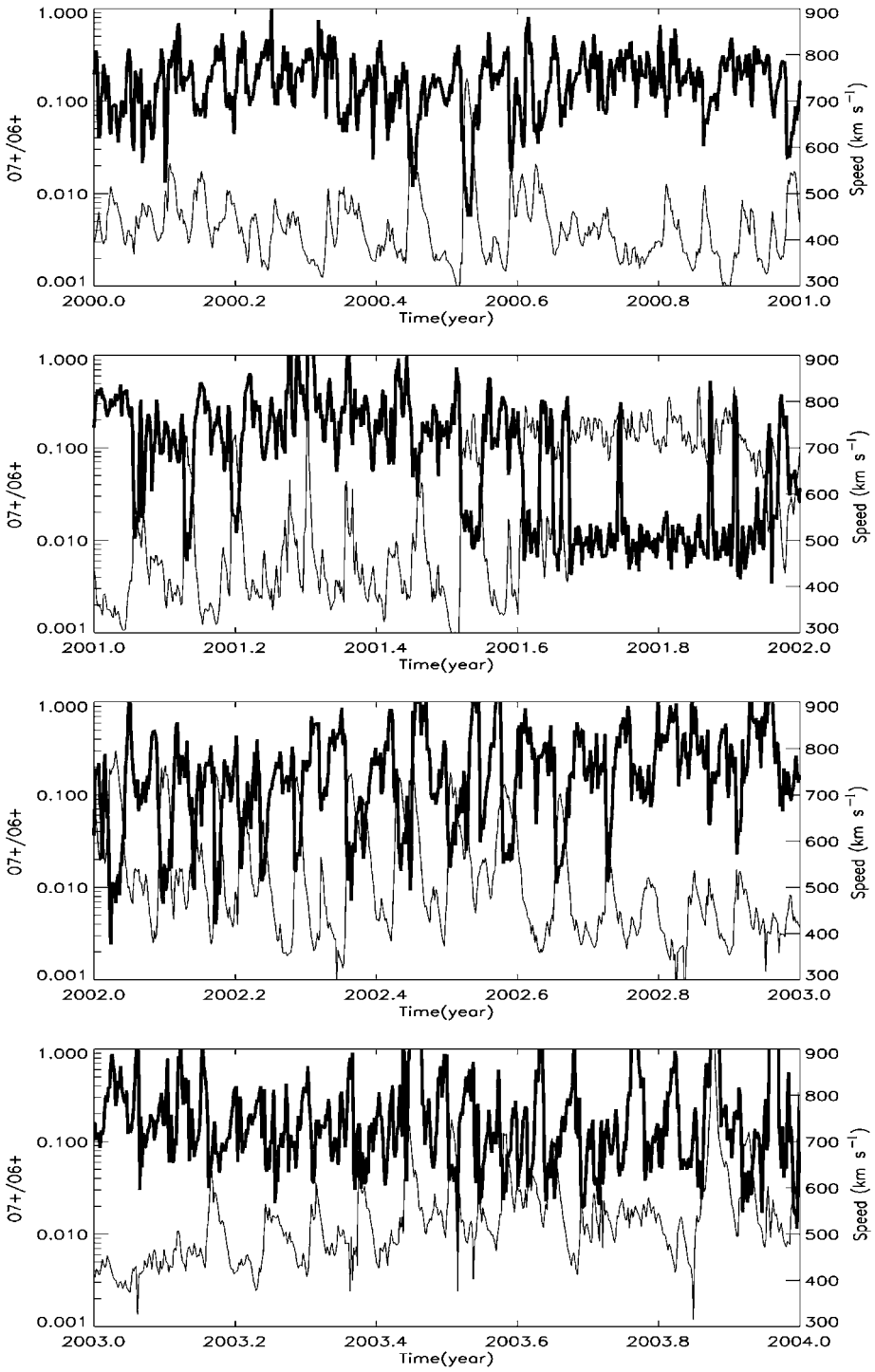

Fig. 1 Solar wind speed (light curve) and O^{7+}/O^{6+} charge-state ratio (heavy) measured by SWICS/Ulysses from 2000 to end-2003, 15-hour averages are displayed.

is higher at 750 to 850 km s^{-1}, compared to typical values of 400 km s^{-1} in the streamer belt. The south and north PCH speeds are about equal. As already reported by McComas et al. (2000) based on Ulysses/SWOOPS data, values averaged over the whole southern (northern) polar stream intervals of solar cycle 22 agree within a few present. For both PCH streams the speed is not constant over the entire coronal hole intervals, rather, it exhibits clear variations (see below). The speed of the solar wind from the northern PCH which newly emerged during the maximum phase of cycle 23 reaches maximum values of 800 km s^{-1}, somewhat less than 850 km s^{-1} encountered at highest latitudes in the northern and southern PCHs of Cycle 22. As already reported by Zhang et al. (2002), the northern PCH of cycle 22 has a significantly lower O^{7+}/O^{6+} charge-state ratio than southern PCH of the same cycle. Translated into coronal temperature this corresponds to a 15% hotter corona in the south. The O^{7+}/O^{6+} charge-state ratio in the north PCH stream of cycle 23 and hence its coronal temperature are as low as the lowest ratio (temperature) encountered in the north PCH.

The coronal hole area, coronal hole net flux and net flux density deduced from the synoptic charts are shown in Figures 2c to 2e. The evolution of the area clearly shows that the northern PCH appeared earlier within the solar cycle than the southern one. In solar cycle 23 the north PCH emerged one year earlier than the south PCH. From 1992 to 1998, the net magnetic flux of the north PCH is slightly lower compared to the south PCH. Furthermore, the net flux densities differ significantly. In the south PCH, the net flux density (in average about −7 Gauss) is nearly 50% larger compared to the north PCH (about 5 Gauss). Due to the magnetic polarity change of the Sun the net flux density of the north and south PCH reversed sign in solar cycle 23. Almost two, (one) year after their formation the level of the flux density still remains considerable below the PCH flux density level of cycle 22.

Figure 3 shows the spatial variations of the properties of coronal hole streams. It presents scatter diagrams of the O^{7+}/O^{6+} ratio (left panel) and the solar wind speed (right panel) plotted against the distance to the polar coronal hole center as derived from the synoptic charts. In order to connect the interplanetary observations with the ground-based synoptic charts, we estimated the solar source location by mapping the interplanetary observation point back to the solar surface. We used a simple ballistic and constant-velocity approach. Observations within three different time intervals are displayed. The time interval from 1992.5 to 1995.0 corresponds to observations within the south PCH during the declining to minimum phase of cycle 22, the period from 1995.0 to 1997.4, to observations within the north PCH during the minimum of cycle 22. Observations from 2001.0 to 2003.6 are from the north PCH, newly emerged during the maximum phase of cycle 23. 'R' represents the radius of a PCH, and 'r', the distance between the location (determined by back-extrapolating the interplanetary observation as described above) on the synoptic map to the center of the PCH. Thus a value of $r/R \ll 1$ points to a location close to the center of the PCH, a value $\sim$1 corresponds to a location close to the boundary. However, we do not take into account a radial expansion of the PCH. Thus the mapping at lower latitudes is less certain. Values of $r/R > 1$ may actually still correspond to locations well within the PCH.

For all three coronal hole streams, a rather strong dependence of the solar wind speed on the distance to the PCH center is observed. The correlation coefficients are −0.71 (−0.94), for the south (north) PCH of cycle 22, and −0.83 for the north PCH of cycle 23. Though the dependence is qualitatively similar, the actual value of the gradient varies considerably. Whereas the evolved PCH of cycle 22 shows a speed decrease of about 30 km s^{-1} (40 km s^{-1}) over the full radius of the PCH, a decrease of more than 100 km s^{-1} is found within the newly emerging PCH of cycle 23.

For the O^{7+}/O^{6+} ratio, the dependence is less pronounced and, moreover, not consistent for the three streams. The south PCH stream of the declining phase of cycle 22 and the north

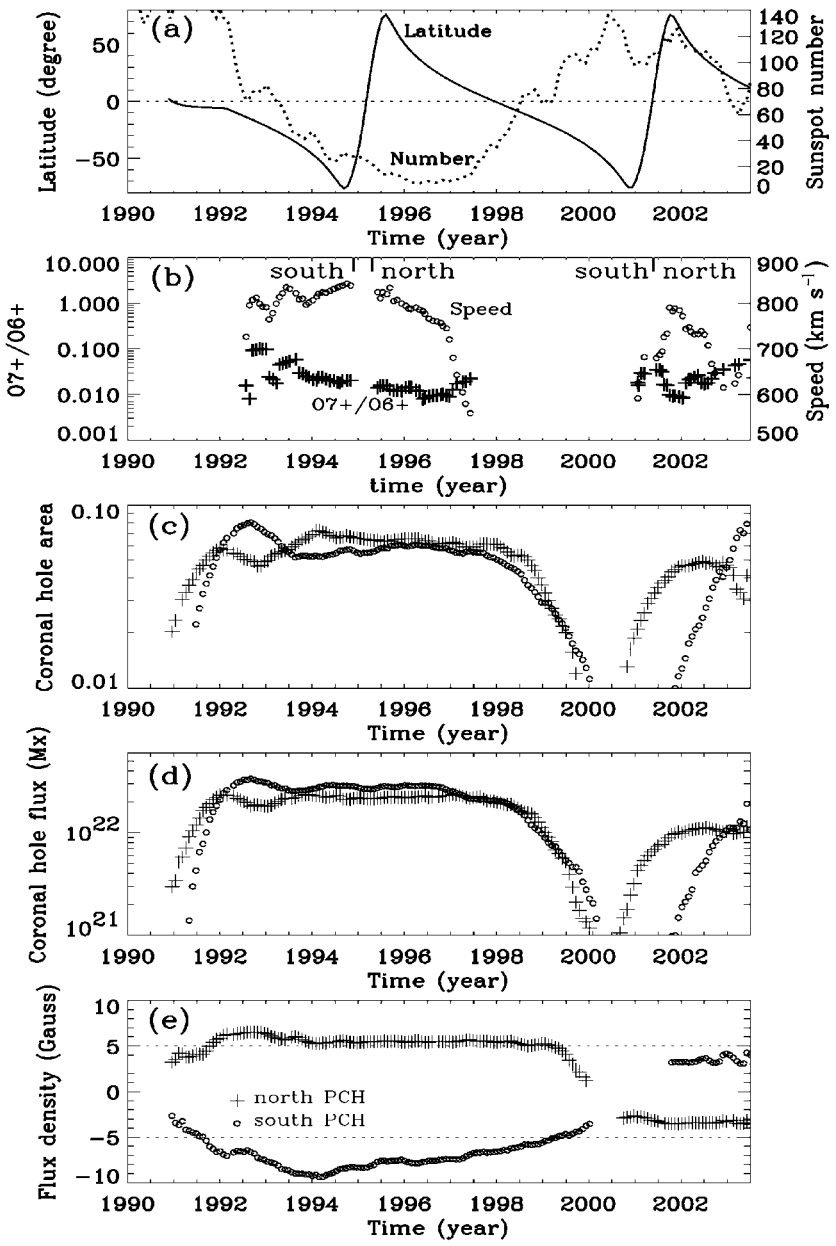

Fig. 2 Selected solar wind and polar coronal hole parameters from 1990 to mid-2003. (a) Heliographic latitude of Ulysses and sunspot number; (b) O^{7+}/O^{6+} ratio and solar wind speed as measured by SWICS/Ulysses; (c) area of the south PCH (∘) and north PCH (+) estimated from Kitt Peak He I 1083 nm synoptic maps as fraction of the solar surface; (d) net magnetic flux of the south (north) PCH derived from Kitt Peak synoptic magnetograms; (e) same as in (d) but for net magnetic flux density.

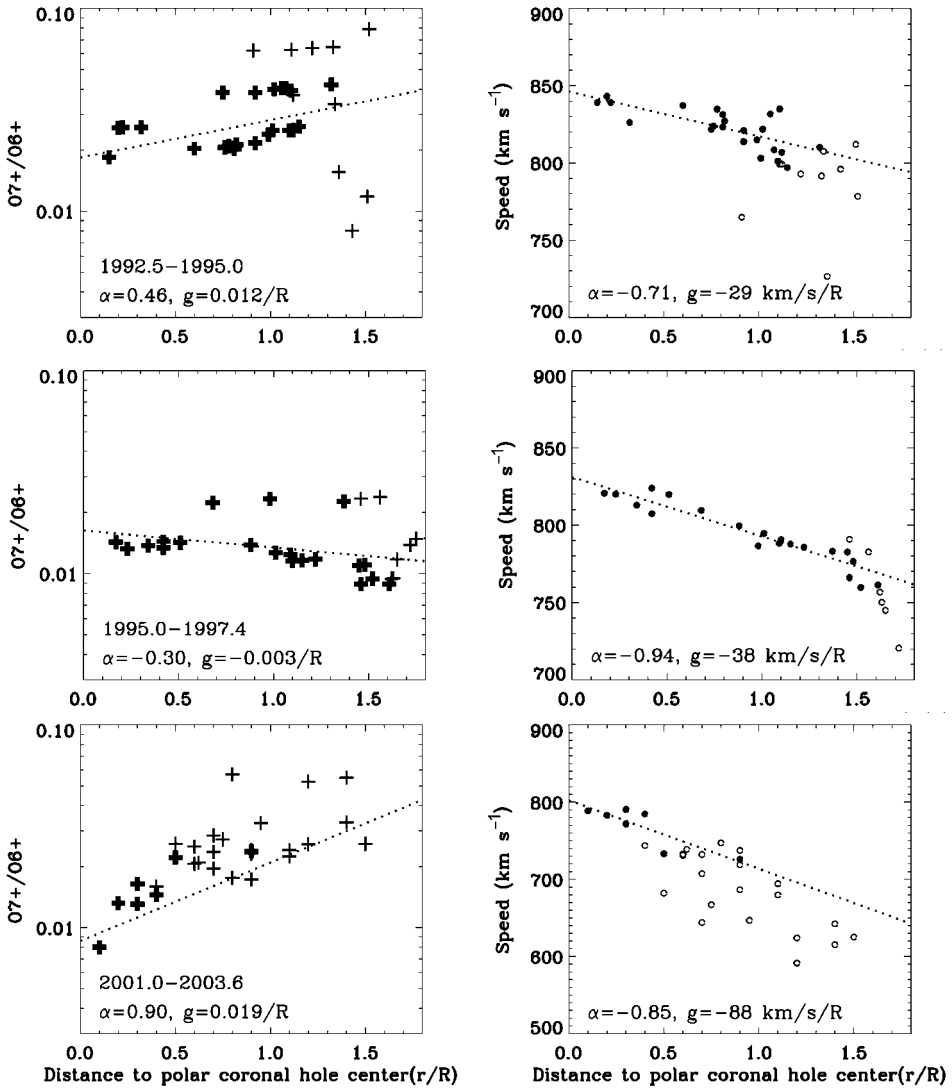

Fig. 3 Center-to-border variations of solar wind speed and O^{7+}/O^{6+} ratio within PCHs (heavy symbols denote pure PCH stream observations, light symbols observations from the fast-slow wind interface regions). Left: O^{7+}/O^{6+} ratio versus distance to polar coronal hole center during 1992.5 to 1995.0 (south PCH, cycle 22) (top), 1995.0 to 1997.4 (north PCH, cycle 22) (middle), and 2001.0 to 2003.6 (north PCH, cycle 23) (bottom). Right: the same but for the solar wind speed.

PCH stream of the maximum phase of cycle 23 show a lowest coronal temperature close to the center of the PCH and a gradual temperature increase towards the boundary. The latitudinal dependence observed in the north PCH stream during solar minimum is less strong and, in contrast, the lowest temperatures are observed at the boundary of the PCH.

3 DISCUSSION

The results presented here confirm previous findings that the solar wind emanating from large-scale polar coronal holes exhibits a pronounced latitude dependence. The solar wind speed peaks at highest latitudes in the center of the PCHs and decreases towards its edges (Neugebauer et al. 1998; McComas et al. 2000; Zhang et al. 2002). In this study, we showed that the latitude dependence is not only found for relatively evolved and spatially extended PCHs, but also for a newly emerging still relatively confined PCH.

Additionally, we noticed that the evolution pattern of the solar wind emanating from the south and north PCH streams depends on the solar cycle in some aspect. For all the confirmed PCHs during the interval 1990 to mid-2003, a correlation between the wind speed and the distance to the PCH center is found. This correlation reflects a latitude dependence. The solar wind speed increases with latitude within the PCH, so that higher values are observed in the center of the PCHs, and lower values at or outside of the edges.

The distribution of the O^{7+}/O^{6+} ratios (usually taken as a proxy for coronal temperatures) observed in interplanetary space is different for young and old PCHs. For a young PCH (appearing at the early declining phase of the cycle), the value of the O^{7+}/O^{6+} ratio increase with the distance to the center of the PCH. On the other hand, for an old PCH (appearing during or after solar minimum), the O^{7+}/O^{6+} ratios show a different variation: higher values in the center of the PCH, and lower, though not pronounced, outside of the edges. It is not fully understandable why young and old PCHs show different frozen-in temperature profiles. We suggest that the O^{7+}/O^{6+} ratio observed in an old PCH cannot yet represent the coronal temperature. Long-time evolutions of an old PCH smooth the temperature distribution in interplanetary space.

Acknowledgements The NSO/Kitt Peak data used here are produced cooperatively by NSF/NOAO, NASA/GSFC, and NOAA/SEL. The maps of coronal holes were prepared by Drs. Karen Harvey and Frank Recely as part of an NSF grant. JZ was supported by the Ministry of Science and Technology of China under Grant G2000078404, NSFC G10243003 and G 10233050. This work was partly supported by the Deutsches Zentrum für Lift-und Raumfahrt e.V.(DLR).

References

Fisk L. A., Zurbuchen T. H., Schwadron N. A., 1999, J. Geophys. Res., 104, 19765
Geiss J., Gloeckler G., von Steiger R. et al., 1995, Science, 268, 1033
Gloeckler G., Geiss J., Balsiger H. et al., 1992, A&AS, 92, 267
Hassler D., Dammasch I. E., Lemaire P. et al., 1999, Science, 283, 810
Krieger A. S., Timothy A. F., Roelof E. C., 1973, Sol. Phys., 29, 505
McComas D. J., Barraclough B. L., Funsten H. O. et al., 2000, J. Geophys. Res., 105, 10419
Neugebauer M., Forsyth R. J., Galvin A. B. et al., 1998, J. Geophys. Res., 103, 14587
Schwenn R., Mülhauser K. H., Rosenbuer H., 1981, in: H. Rosenbauer, ed., Solar Wind Four, 118
von Steiger R., Geiss J., Gloeckler G., 1997, in: J. R. Jokipii et al., eds., Cosmic Winds and the Heliosphere, Univ. of Ariz. Press, 581
von Steiger R., Schwadron N. A., Fisk L. A., et al., 2000, J. Geophys. Res., 105, 27217
Woch J., Axford W. I., Mall U. et al., 1997, Geophys. Res. Lett., 24, 2885
Zhang J., Woch J., Solanki S. K., von Steiger R., 2002, Geophys. Res. Lett., 29, 1236
Zhang J., Woch J., Solanki S. K., von Steiger R., Forsyth R., 2003, J. Geophys. Res., 108, 1144
Zurbuchen T. H., Fisk L. A., Gloeckler G., von Steiger R., 2002, Geophys. Res. Lett., 29, 1352